LBL-22504
Preprint c.2

Lawrence Berkeley Laboratory
UNIVERSITY OF CALIFORNIA

Materials & Chemical Sciences Division

RECEIVED
LAWRENCE
BERKELEY LABORATORY

JUN 9 1987

DOCUMENTS SECTION

Submitted for publication

IN SITU OBSERVATIONS OF THE EFFECT OF DOPANTS ON THERMAL OXIDATION OF GALLIUM ARSENIDE

O.R. Monteiro and J.W. Evans

December 1986

TWO-WEEK LOAN COPY
This is a Library Circulating Copy
which may be borrowed for two weeks.

LBL-22504 c.2

Prepared for the U.S. Department of Energy under Contract DE-AC03-76SF00098

DISCLAIMER

This document was prepared as an account of work sponsored by the United States Government. While this document is believed to contain correct information, neither the United States Government nor any agency thereof, nor the Regents of the University of California, nor any of their employees, makes any warranty, express or implied, or assumes any legal responsibility for the accuracy, completeness, or usefulness of any information, apparatus, product, or process disclosed, or represents that its use would not infringe privately owned rights. Reference herein to any specific commercial product, process, or service by its trade name, trademark, manufacturer, or otherwise, does not necessarily constitute or imply its endorsement, recommendation, or favoring by the United States Government or any agency thereof, or the Regents of the University of California. The views and opinions of authors expressed herein do not necessarily state or reflect those of the United States Government or any agency thereof or the Regents of the University of California.

LBL-22504

IN SITU OBSERVATIONS OF THE EFFECT OF DOPANTS ON THERMAL OXIDATION OF GALLIUM ARSENIDE

O. R. Monteiro*

and

J. W. Evans†

Materials and Chemical Sciences Division
Lawrence Berkeley Laboratory and
Department of Materials Science and Mineral Engineering
University of California
Berkeley, CA 94720

*Graduate student.

†Professor of Metallurgy, to whom correspondence should be addressed.

ABSTRACT

The thermal oxidation of GaAs has been studied using in situ transmission electron microscopy and secondary ion mass spectroscopy. Four different materials, i.e. undoped, chromium, silicon and tellurium doped were considered, and their different behavior upon oxidation can be explained in terms of dopant redistribution between oxide and semiconductor phases. Chromium doped samples resulted in the slowest oxidation rate. In all cases, oxidation appears to initially form epitaxial γ-Ga_2O_3 and subsequently polycrystalline β-Ga_2O_3 while some of the As volatilizes after being oxidized and some accumulates at the semiconductor/oxide interface.

INTRODUCTION

Oxidation of gallium arsenide is a topic of potential interest to the semiconductor industry since (by analogy with silicon oxidation) the ability to easily produce homogeneous and uniform oxide layers would facilitate the manufacture of devices based on GaAs.

Three methods of oxidation have been discussed in the literature (1-4): plasma, anodic and thermal oxidation. One of the first publications to examine the thermal oxidation of GaAs was that of Minden (9) and several investigations have followed, using a variety of experimental techniques to characterize the phases formed during oxidation. The majority of these publications are consistent with the following description of the oxidation.

At low temperatures, i.e. below approximately 400°C, the oxidation product is amorphous. Polycrystalline β-Ga_2O_3 forms when oxidation is carried out at intermediate temperatures (400°C - 700°C approximately) and a mixture of $GaAsO_4$ and β-Ga_2O_3 forms at higher temperatures. Recently, questions have been raised about the product phase in the intermediate temperature range (8,12); γ-Ga_2O_3 having been observed along with β-Ga_2O_3 in these studies.

The fate of arsenic has been disputed. Wilson (4) suggested that As may diffuse out through the oxide layer, perhaps through grain boundaries, thus explaining the absence of arsenic at the oxide-GaAs interface (1,9,11). Other studies found segregation of arsenic at the interface but disagreed on whether it would be present in an elemental form (12), or as an oxide (13).

The present study was concerned with thermal oxidation and this report presents some results obtained by in-situ transmission electron microscopy. This technique has been used (5-7) to study other reactions, but, apart from a preliminary study (8), has not been applied to the oxidation of GaAs. Secondary ion mass spectroscopy was used to obtain information on in-depth concentration profiles of oxidized GaAs. The paper describes experiments using Te doped, Si doped, Cr doped and undoped gallium arsenide. No previous work has examined the effect of doping elements on the oxidation of GaAs.

EXPERIMENTAL PROCEDURE

The in-situ oxidation studies were carried out using the Hitachi HU 650 and the KRATOS EM 1500 high voltage transmission electron microscopes at Lawrence Berkeley Laboratory. These microscopes are equipped with an environmental cell described previously (8). These experiments were supplemented with conventional electron microscopy where necessary.

SIMS analyses were carried out at Charles Evans and Associates (Redwood City, CA). Oxygen ion bombardment and positive secondary ion mass spectrometry was employed to obtain Cr, O and As concentration profiles in the Cr doped GaAs. Cesium ion bombardment and negative secondary ion mass spectrometry were used to profile O, As and either Si or Te in respectively doped samples. The concentration scales are based on relative sensitivity factors derived from previously analysis of ion implanted GaAs standards. This calibration is accurate to

within a factor of two. The O and As profiles have been plotted on ion intensity scales to serve as markers of the oxide layers, and provide no quantitative information. The depth scales for all the profiles are calibrated with stylus profilometer measurements of the sputtered craters.

Gallium arsenide specimens were prepared from (100) wafers supplied by Hewlett-Packard and Morgan Semiconductor. Four types of wafers were used in the in-situ experiments: Te doped (2×10^{18} cm^{-3}, HP), Si doped (2.2×10^{18} cm^{-3}, HP), Cr doped (3×10^{15} cm^{-3}, MS), and undoped (MS). For the in-situ experiments, wafers were thinned by polishing on emery paper followed by 6μm and 1μm diamond pastes. Three millimeter disks were cut from polished foil and a dimple made on one side. Final thinning to perforation was by a 1% bromine in methanol solution. The samples which were analyzed for in-depth concentration profiles were oxidized in a quartz tubular furnace at atmospheric pressure. Oxygen, direct from a cylinder, was used in both cases.

RESULTS

Silicon doped GaAs

In initial experiments samples were held at 400°C and total pressure below 10^{-5} torr to determine whether vaporization at the elevated temperatures would be discernible. Although no gross vaporization of the samples occurred there was sufficient residual oxygen at this low pressure to produce a thin layer of polycrystalline

β-Ga_2O_3 covering the original GaAs (Figure 1). The dark spots which appeared during the oxidation could not be identified here but results described below suggest they are some arsenic compound which is produced as a consequence of the oxidation reaction.

Oxidation experiments were then carried out at 400°C and 500°C, both with 10 torr of oxygen. At this pressure, the reaction at 400°C was fast enough so that enough As_2O_5 was formed to be detected in the diffraction pattern shown in Figure 2, which indicates also the presence of β-Ga_2O_3 and GaAs . The oxidation can therefore be represented by

$$2GaAs + 4O_2 = \beta\text{-}Ga_2O_3 + As_2O_5 \qquad (1)$$

As will be discussed below, the phenomena actually involved in the oxidation may be more complicated than represented in this simple equation.

At 500°C a reaction similar to [1] occurred but epitaxial γ-Ga_2O_3 was also found with a unique orientation relationship with respect to the GaAs. This is shown in Figure 3 from which it can be seen that

$$[001]_{GaAs} \quad // \quad [001]_{\gamma\text{-}Ga_2O_3}$$

$$(110)_{GaAs} \quad // \quad (110)_{\gamma\text{-}Ga_2O_3}$$

This result is in agreement with the one found by Sands et al. (12) after oxidation of Si doped GaAs.

As_2O_5 was detected, also at 500°C, in the oxide layer near the sample edges. It appears as precipitates in the Ga_2O_3 matrix as the dark field image in Figure 4 reveals.

Two alternative reaction schemes can be suggested for the oxidation at 500°C .

$$\begin{array}{ccccc} 2GaAs & + & 4O_2 & \longrightarrow & \text{polycrystalline } \beta\text{-}Ga_2O_3 + As_2O_5 \\ \downarrow & & & & \uparrow \\ \text{epitaxial } \gamma\text{-}Ga_2O_3 & & & \longrightarrow & \text{polycrystalline } \gamma\text{-}Ga_2O_3 \end{array} \qquad [2a]$$

$$\begin{array}{ccccc} 2GaAs & + & 4O_2 & \longrightarrow & \beta\text{-}Ga_2O_3 + As_2O_5 \\ \downarrow & & & & \\ \text{epitaxial } \gamma\text{-}Ga_2O_3 & & & \dashrightarrow & \text{polycrystalline } \gamma\text{-}Ga_2O_3 \end{array} \qquad [2b]$$

In [2b] the β-Ga_2O_3 is formed directly from GaAs whereas in [2a] it is formed (at least in part) by transformation of γ-Ga_2O_3.

In-depth concentration profile of oxidized Si doped GaAs (from HP) are given in Figure 5 for two oxidation temperatures. Despite the impossibility of accurately determining the thickness of the oxide it can be estimated from the position of the As peaks, which occurs at the semiconductor side of the GaAs/oxide interface.

Tellurium doped GaAs

TEM results with this material were virtually identical to those obtained from Si doped GaAs when oxidation was carried out at 400°C and 500°C. Again an amorphous phase was formed in oxidation at lower temperatures (310°C), consistent with the results of Bull and Sealy (12). The nature of the oxide present could not be determined

unambiguously because all the polymorphs of gallium oxide and arsenic oxide have intense lines with d-spacings lying within the broad amorphous rings of the electron diffraction pattern.

SIMS results are shown in Figure 6 and a comparison between Figures 5 and 6 indicate that the oxide thickness is smaller in the oxidation of Te doped material. In the Te case, the dopant tends to accumulate in the oxide, with its concentration increasing up to an order of magnitude with respect to the original GaAs.

Undoped GaAs

Oxidation of undoped gallium arsenide at 400°C and 10 torr oxygen pressure resulted in the formation of very little β-Ga_2O_3 and an amorphous oxide. Such amorphous product was not detected during the oxidation of Si doped and Te doped GaAs under these conditions.

At 500°C and 10 torr of oxygen (Figure 7), reaction yields products according to [2a] or [2b]. The dark precipitates in the oxide layer, particularly in the vicinity of the oxide-semiconductor interface, are found to be As_2O_5 from the diffraction pattern. In-situ TEM indicates a substantially faster oxidation at 600°C (Figure 8), the reaction proceeding via formation of γ-Ga_2O_3 and β-Ga_2O_3 with small amounts of As_2O_5.

Chromium doped GaAs

Oxidation of chromium doped gallium arsenide proceeded differently from the oxidation of the materials described above. Formation of gallium oxides followed the routes of [2a] and [2b] described earlier but, instead of the production of As_2O_5 alone, a

combination of As_2O_5, As_2O_3 and As was obtained depending on the oxidation conditions.

Figure 9, obtained at 500°C and 20 torr of oxygen, shows As_2O_3 mixed with epitaxial γ-Ga_2O_3 and some polycrystalline β-Ga_2O_3 produced after 80 minutes of oxidation. The As_2O_3 appears as the bright areas in the dark field image of Figure 9. Figure 10 shows another region of the same specimen where arsenic is present as As_2O_5. Crystalline arsenic was also found in this same example (Figure 11).

Oxidation at 600°C and 20 torr of oxygen also resulted in a mixture of β- and γ-Ga_2O_3 as well as As_2O_5, As_2O_3 and precipitates of As at the semiconductor-oxide interface (Figure 12). In contrast to a previous investigation (13) which used lattice imaging, a unique orientation between hexagonal As and GaAs was not found. Large As precipitates were identified with at least two different orientation relationships with the matrix.

SIMS results for the chromium doped GaAs oxidized at 500°C and 600°C and 1 atm oxygen are shown in Figure 13. Comparing Figures 5, 6, and 13 one notices that the chromium doped samples were the ones to produce the thinnest oxide layer. Chromium also has a tendency to migrate toward the outermost oxide layer during oxidation. Chromium concentration was not uniform in the wafers even prior to oxidation; it showed a remarkable increase at the free surface. One could think this effect arose from the technique used to analyze the samples, but the results of the oxidized samples showed that this was not the case.

In fact the chromium rich region increased with the oxidation time and temperature as Figures 13b and 13c show.

DISCUSSION

Not much difference was found between the behavior of the undoped, silicon doped and tellurium doped gallium arsenide regarding the nature of the product phases. The oxide layer however is thicker in the Si doped than in the Te doped GaAs. No thickness estimate is available for the undoped material.

Oxidation of Cr doped GaAs yielded products which have not been detected in the other cases and a much thinner oxide layer, i.e. about 5 times smaller than the oxide of Te doped GaAs or 10 times smaller than the one of Si GaAs. Table I summarizes the similarities and differences between the behavior of the four types of GaAs. Previous investigations of GaAs oxidation have neglected the effect of doping elements and this may be a reason for the discrepancy between some reported results.

Regarding the arsenic product phases, no previous investigation has reported the formation of As_2O_5. A pseudo ternary diagram (16) for the system Ga-As-O, determined at low temperatures, fails to predict As_2O_5.

Free energies of several reactions that might occur during the oxidation process are presented in Table II. These values were calculated from data available in the literature (17). The table also contains the calculated oxygen pressures at equilibrium for each

reaction. These calculations were carried out assuming that the other species in the reaction were present at unit activity. One can notice that the oxygen pressures used in this investigation are sufficient to bring about complete oxidation of GaAs to Ga_2O_3 and As_2O_5 if kinetics allows. The appearance of lower oxides or elemental arsenic is therefore due to either:

[i] kinetic effects due to depletion of one or more of the reactants or

[ii] reactions [6] and [7] in those regions where GaAs is in contact with an oxide and the oxygen pressure is low.

Both hypotheses should lead to a structure that is more highly oxidized at exterior surfaces, which is consistent with experimental observations.

The mechanism governing the thermal oxidation of gallium arsenide is still unclear. Wilsen (20) believed that the reaction at the semiconductor/oxide interface plays an important role and the breakage of GaAs bonds is the rate determining step. However, since the diffusing species are not known (O, Ga or As) the complete model for growth remains uncertain. Sugano (25) deduced that the rate limiting step below 700°C is the migration of O. In this case accumulation of As at the interface is caused by preferential oxidation of Ga as Table II suggests.

In spite of the dispute regarding the correct oxidation mechanism, some kinetic studies of the reaction have been made (4,21). Butcher and Sealy (4) used Rutherford backscattering spectroscopy to

conclude that oxidation follows a parabolic law at low oxide thickness and becomes linear as the oxide thickens. Earlier, Murarka (21) had found only a linear regime. The physical models proposed to explain these kinetic results (e.g. diffusion through oxide grain boundaries or diffusion through the oxide layer), as formulated, do not have a strong dependence on the dopant element, and therefore do not explain the results presented here.

An analysis of the oxide characteristics sheds some light on the problem allowing an improvement in the understanding of the process. Ga_2O_3 is an n-type oxide (22,23) with free carriers apparently due to anion vacancies (22). Thus the overall oxidation reaction can be broken into:

$$V_O^{\cdot\cdot} + 1/2\ O_2\ (g) + 2\ e^- \longrightarrow O_O^x$$

at the oxide/oxygen interface and

$$GaAs \longrightarrow Ga^{3+} + (As^{3+}) + 6e^-$$

at the oxide/GaAs interface. Here the Kroger notation for point defects is used. In order for the oxide film to grow, the positive ions and electrons must migrate to the oxide/oxygen interface. Since the dopant levels in the oxidized GaAs are so small it is most likely that their effect results from altering the conductivity of the oxide rather than its chemical properties. Additions of substitutional Si or Te to Ga_2O_3 result in an increase of the conductivity because of the increase in electron concentration according to Hauffe's rule (24). The effect of chromium however is not as straightforward. Being a Ga^{3+} isovalent ion its effect cannot be explained on the same

basis. Chromium is a transition metal and even as Cr^{3+} still has an incomplete d-shell. Thus it may result in electron traps which reduce the conduction electron concentration and consequently the conductivity. Another possible explanation for the decreased kinetics of the Cr doped samples is the fact that Cr enrichment at the surface may increase the impermeability of the oxide layer, due to chromium oxide formation. No such oxide was detected in this investigation.

Another observation to be discussed is the effective decrease of the oxide thickness with increasing temperature as noticed from the SIMS in-depth oxygen profiles. It can be attributed to the vaporization of As or its oxides which becomes much greater at higher temperatures. Thus an increase in the oxidation rate does not necessarily correspond to an increase in oxide thickness. Figures 5, 6 and 13c show that oxidation of the Si doped, Te doped and a very long oxidation of the Cr doped GaAs in fact resulted in substantial loss of arsenic in the oxide. For the short term oxidation at 500°C of Cr doped GaAs such depletion is not evident (Figure 13a and 13b).

CONCLUSIONS

Thermal oxidation of undoped and chromium, tellurium and silicon doped GaAs was studied using in-situ transmission electron microscopy and secondary ion mass spectroscopy. The sequential formation of β-Ga_2O_3 with intermediate polycrystalline and epitaxial γ-Ga_2O_3 was confirmed for all dopants at an intermediate oxidation temperature (between 450°C and 600°C). Within this temperature range, the upper

limit favors a more homogeneous oxide layer due to As loss. SIMS in-depth concentration profiles indicate that under these conditions a more abrupt oxide/semiconductor interface is formed. At temperatures below 400°C an amorphous oxide layer is formed which is probably a mixture of arsenic and gallium oxides.

The results described here support the overall idea that Ga is preferentially oxidized while As is rejected ahead of the interface (Figure 5, 6 and 13) so that it accumulates to a point where it starts to either precipitate, oxidize or both. Due to their high vapor pressures, arsenic oxides readily volatilize.

Although there is still some uncertainty concerning the overall mechanism of oxidation and the rate determining step, the observed effect of doping elements on the process highlights the importance of electron transport through the oxide.

ACKNOWLEDGMENT

The authors would like to express their gratitude for helpful discussions with Profs. Eicke Weber and Tom Devine. One of the authors (ORM) acknowledges a fellowship from CAPES (Coordenação de Aperfeiçoamento de Pessoal de Nivel Superior), Brazil. This work was supported by the Director, Office of Energy Research, Office of Basic Energy Sciences, Materials Sciences Div. of the U.S. Dept. of Energy under Contract no. DE-AC03-76SF00098.

REFERENCES

1) S. J. Long, B. M. Welch, R. Zucca and R. C. Eden, J. Vac. Sci. Technol. 19, 531 (1981).

2) K. Watanabe, M. Hashiba, Y. Hirshata, M. Nishino and T. Yamashima, Thin Solid Films 56, 53 (1979).

3) C. W. Wilson, R. W. Kee and K. M. Geib, J. Vac. Sci. Technol. 16, 1434 (1979).

4) D. N. Butcher and B. J. Sealy, J. Phys. D: Appl. Phys 11, 1451 (1978).

5) C. W. Wilsen, Thin Solid Films 39, 105 (1976).

6) H. M. Flower and P. R. Swann, Act. Metall. 22, 1339 (1974).

7) D. A. Goulden, Phil. Mag. 33 393 (1976).

8) H. M. Flower and B. A. Wilcox, Corros. Sci. 17, 253 (1977).

9) M. Hall, M. F. Rau and J. W. Evans, J. Electrochem. Soc. 133, 1939 (1986), LBL-20839.

10) H. T. Hinden, J. Electrochem. Soc. 109, 733 (1962).

11) A. V. Emelyanov, A. V. Nikitin, V. Timofeev and A. N. Shoken, Sov. Phys. Crystallog. 20, 373 (1975).

12) C. J. Bull and B. J. Sealy, Phil. Mag. 37, 489 (1978).

13) T. Sands, J. Washburn and R. Gronsky, LBL Report # 18636 (1984).

14) Y. Mizobawa, H. Iwasaki, R. Nishitani and S. Nakamura, Jpn. J. Appl. Phys. 17, 327 (1978).

15) O. V. Romanov, Rev. Phys. Appl. 19, 389 (1984).

16) C. D. Thurmond, G. P. Schwartz, G. W. Kammlot and B. Schwartz, J. Electrochem. Soc. 127, 1366 (1980).

17) R. C. Weast (ed.), CRC Handbook of Chemistry and Physics, 65th ed., CRC Press Inc., Boca Raton, Florida (1985).

18) M. E. Greiner, Ph.D. Thesis, Stanford University (1984).

19) M. D. Deal, Ph.D. Thesis, Stanford University (1983).

20) C. W. Wilsen, J. Vac. Sci. Technol., 19, 279 (1983).

21) S. P. Murarka, Appl. Phys. Lett. 26, 180 (1975).

22) M. R. Lorentz, J. F. Woods and R. J. Gambino, J. Phys. Chem. Solids 28, 403 (1967).

23) F. Eba and P. Gode, C. R. Acad. Sc. Paris, 291, 61 (1980).

24) K. Hauffe, *Oxidation of Metals*, Plenum Press, New York (1965).

25) T. Sugano, Thin Solid Films 72 , 9-17 (1980).

FIGURE CAPTIONS

Figure 1: In-situ thermal annealing of Si doped GaAs at 400°C. Total pressure below 10^{-5}T. Annealing times are given in minutes at the top of each pressure. β-Ga_2O_3 was detected after about 30 min.

Figure 2: GaAs:Si oxidized at 400°C, p_{O_2} = 10T for 60 minutes. Bright field (BF) and dark field (DF) images are shown with the diffraction pattern obtained from the center of the picture. Arrow in DP shows the reflection used to obtain DF image. Rings are As_2O_5 reflections superimposed on β-Ga_2O_3 and spots are GaAs with zone axis <100>.

Figure 3: Diffraction pattern of Si doped GaAs after being oxidized for 15 min. at 500°C in 10T O_2. It shows a unique relationship established between GaAs and γ-Ga_2O_3.

Figure 4: Si doped GaAs oxidized at 500°C, p_{O_2} = 10T for 45 min. Dark field imaged with As_2O_5 indicated. Bright areas in DF highlight the As_2O_5 crystals.

Figure 5: SIMS in-depth profile of Si doped GaAs oxidized for 2 hrs at 1 atm O_2 and a) 500°C b) 600°C.

Figure 6: SIMS in-depth profile of Te doped GaAs oxidized for 2 hrs at 1 atm O_2 and a) 500°C b) 600°C.

Figure 7: In-situ thermal oxidation of undoped GaAs at 500°C and 10T O_2. Times are given in minutes at the top left side of each bright field image. Diffraction patterns with arrows show the regions wherefrom they were obtained. An epitaxial relationship between GaAs and γ-Ga_2O_3 is noted in DP at 20 min and the rings of As_2O_5 are detected in DP at 55 min.

Figure 8: In-situ thermal oxidation of undoped GaAs at 600°C and 10T O_2. Times in minutes are given on the top right side of each picture.

Figure 9: Cr doped GaAs oxidized at 500°C, P_{O_2} = 20T for 45 min. The oxide layer near the edge of the sample consists of epitaxial γ-Ga_2O_3 and As_2O_3 as the DP shows. The DF was obtained with a As_2O_3 reflection indicated by the arrow.

Figure 10: Another area of same specimen shown in Figure 9. Complete oxidation occurred here to γ-Ga_2O_3 and very little As_2O_5.

Figure 11: Elemental As (hex.) found at the oxide/GaAs interface after oxidation at 500°C and 20T of Cr doped GaAs.

Figure 12: Cr doped GaAs oxidized at 600°C and 20T O_2 for 10 min. Diffraction pattern of the lettered areas are provided for identification of the prevailing phases.

Figure 13: SIMS in depth profile of Cr doped gallium arsenide oxidized at 1 atm O_2 and a) 500°C for 20 min; b) 500°C for 2 hrs; c) 600°C for 24 hrs.

TABLE I

Summary of Experimental Observations

Material	Temperature	Reaction Products
GaAs, GaAs:Si, GaAs:Te	$\leq 400^{\circ}C$	amorphous oxides
	$400^{\circ}C$ - $500^{\circ}C$	poly x-tal β-Ga_2O_3 + amorphous oxides
	$\geq 500^{\circ}C$	poly x-tal β-Ga_2O_3, γ-Ga_2O_3, As_2O_5
GaAs:Cr	$\leq 400^{\circ}C$	amorphous oxide
	$400^{\circ}C$ - $500^{\circ}C$	poly x-tal β-Ga_2O_3 + amorphous oxide
	$\geq 500^{\circ}C$	poly x-tal β-Ga_2O_3 + γ-Ga_2O_3 + As + As_2O_3 + As_2O_5

TABLE II

Free energy of reaction (kJ)

and equilibrium partial oxygen pressure, where applicable (Torr)

Reaction	T = 400°C	500°C	600°C
$2GaAs + 4O_2 = Ga_2O_3 + As_2O_5$ [3]	-1325	-1245	- 1166
	(1.3×10^{-24})	(6.8×10^{-19})	(2.3×10^{-15})
$2GaAs + 3O_2 = Ga_2O_3 + As_2O_5$ [4]	-1212	-1157	-1103
	(3.8×10^{-29})	(6.1×10^{-24})	(7.6×10^{-20})
$2GaAs + \frac{3}{2} O_2 = Ga_2O_3 + 2As$ [5]	- 735	- 702	- 672
	(6.8×10^{-36})	(1.5×10^{-29})	(7.6×10^{-25})
$2GaAs + As_2O_3 = Ga_2O_3 + 4As$ [6]	- 259	- 246	- 242
$2GaAs + \frac{3}{5}As_2O_5 = Ga_2O_3 + \frac{16}{5} As$ [7]	- 382	- 377	- 377
$2GaAs + 3As_2O_5 = Ga_2O_3 + 4As_2O_3$ [8]	- 873	- 894	- 915

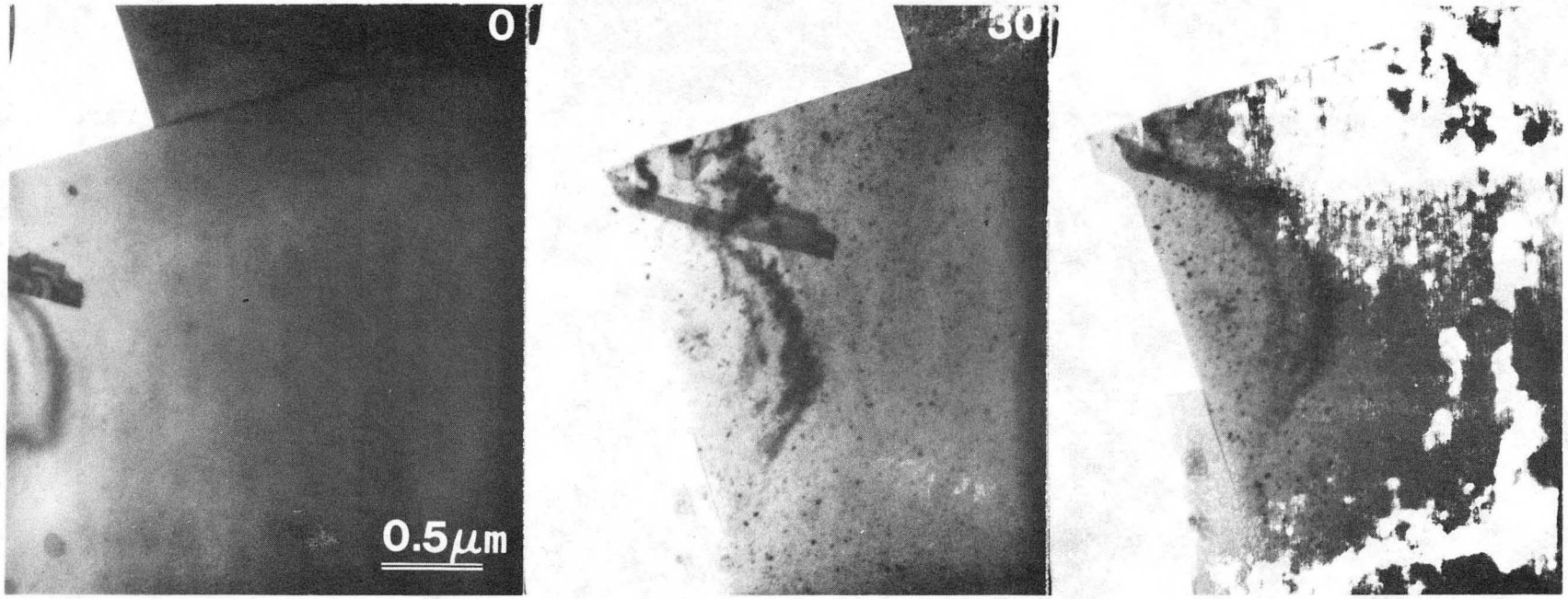

CB 869-7871

Fig. 1

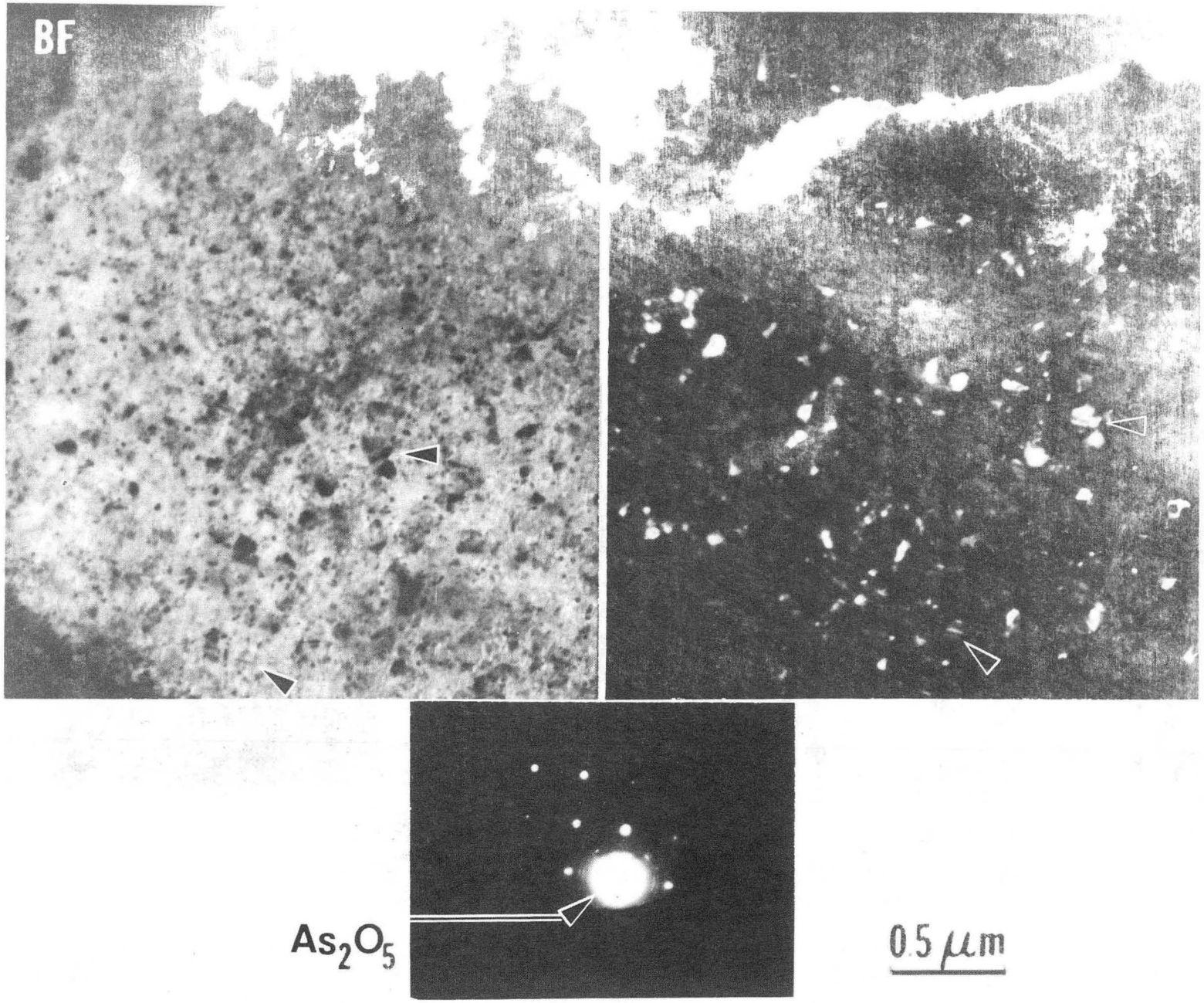

XBB 869-7883

Fig. 2

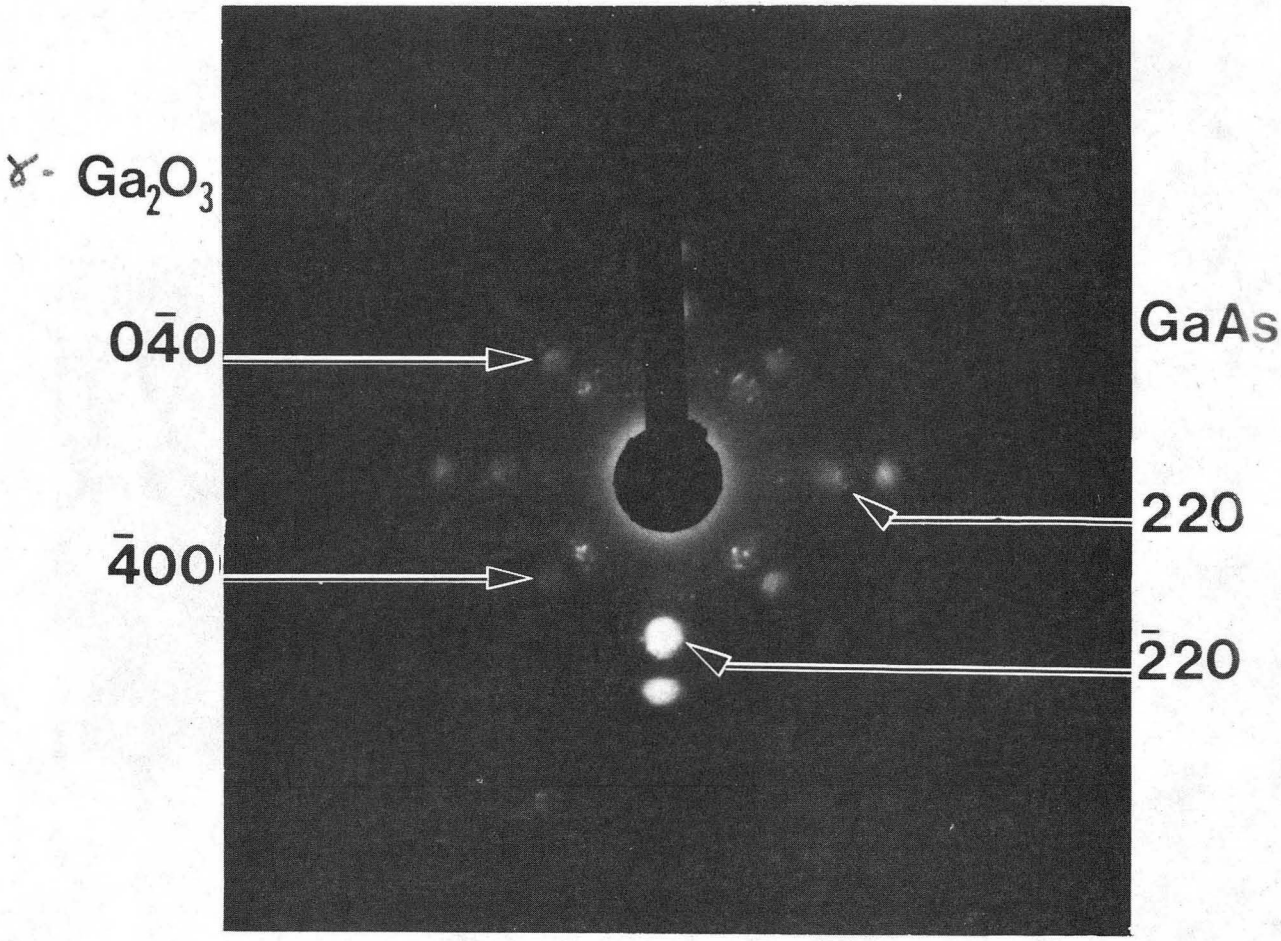

XBB 869-7882

Fig. 3

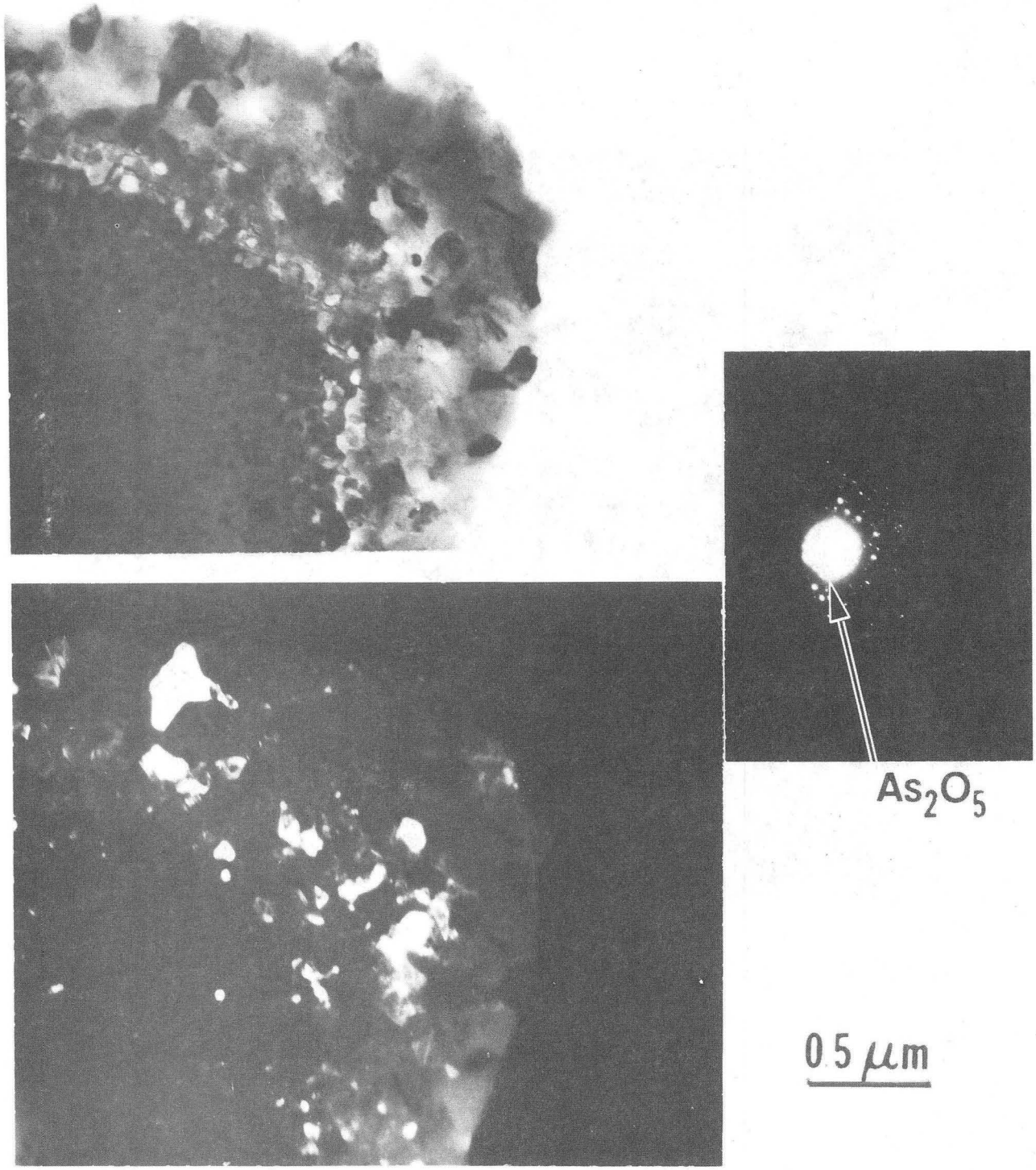

XBB 869-7879

Fig. 4

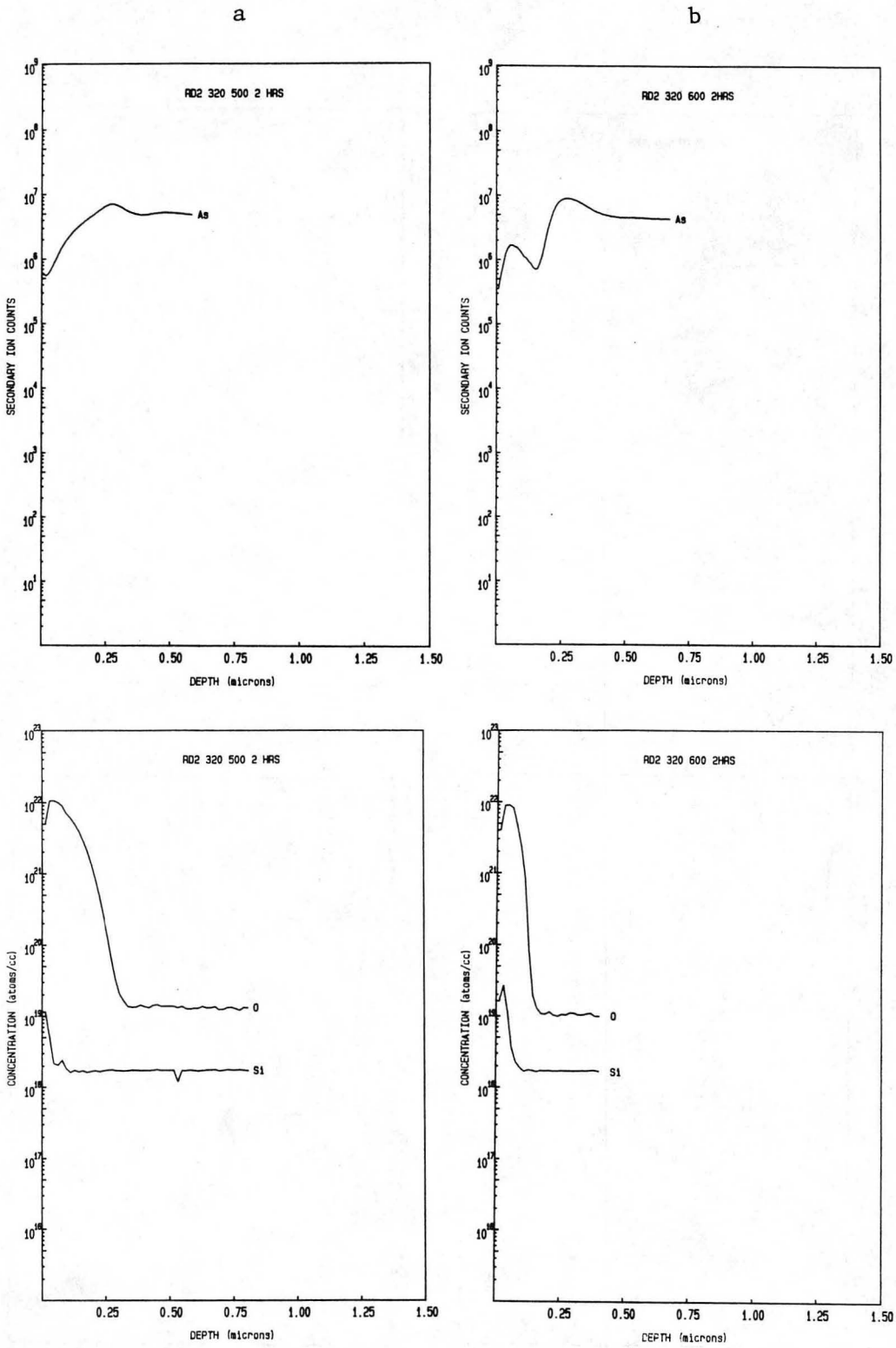
a
b
RD2 320 500 2 HRS
RD2 320 600 2HRS
As
SECONDARY ION COUNTS
DEPTH (microns)
0.25
0.50
0.75
1.00
1.25
1.50
O
S1
CONCENTRATION (atoms/cc)

Fig. 5

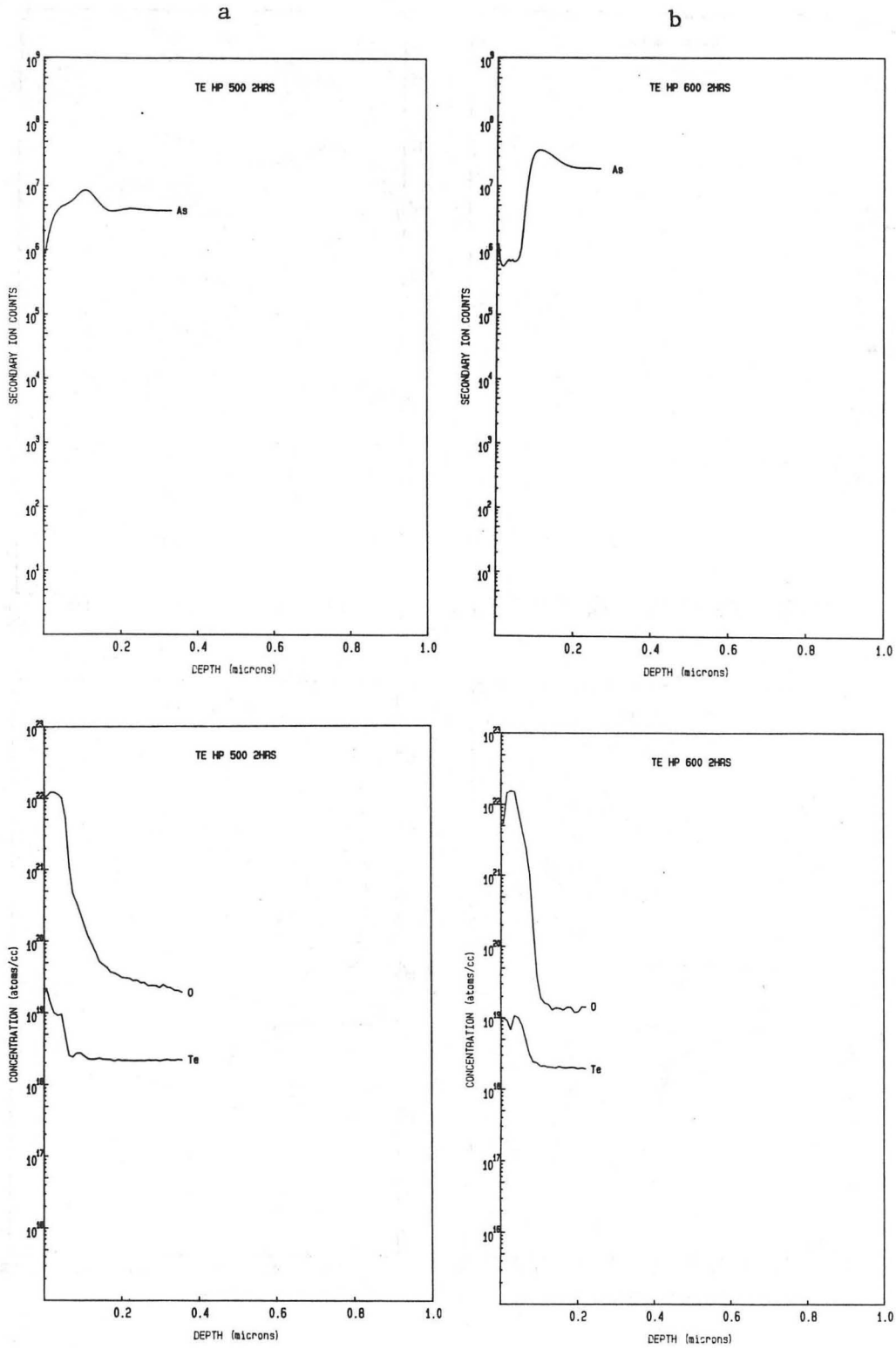
a
b
TE HP 500 2HRS
TE HP 600 2HRS
As
SECONDARY ION COUNTS
DEPTH (microns)
O
Te
CONCENTRATION (atoms/cc)

Fig. 6

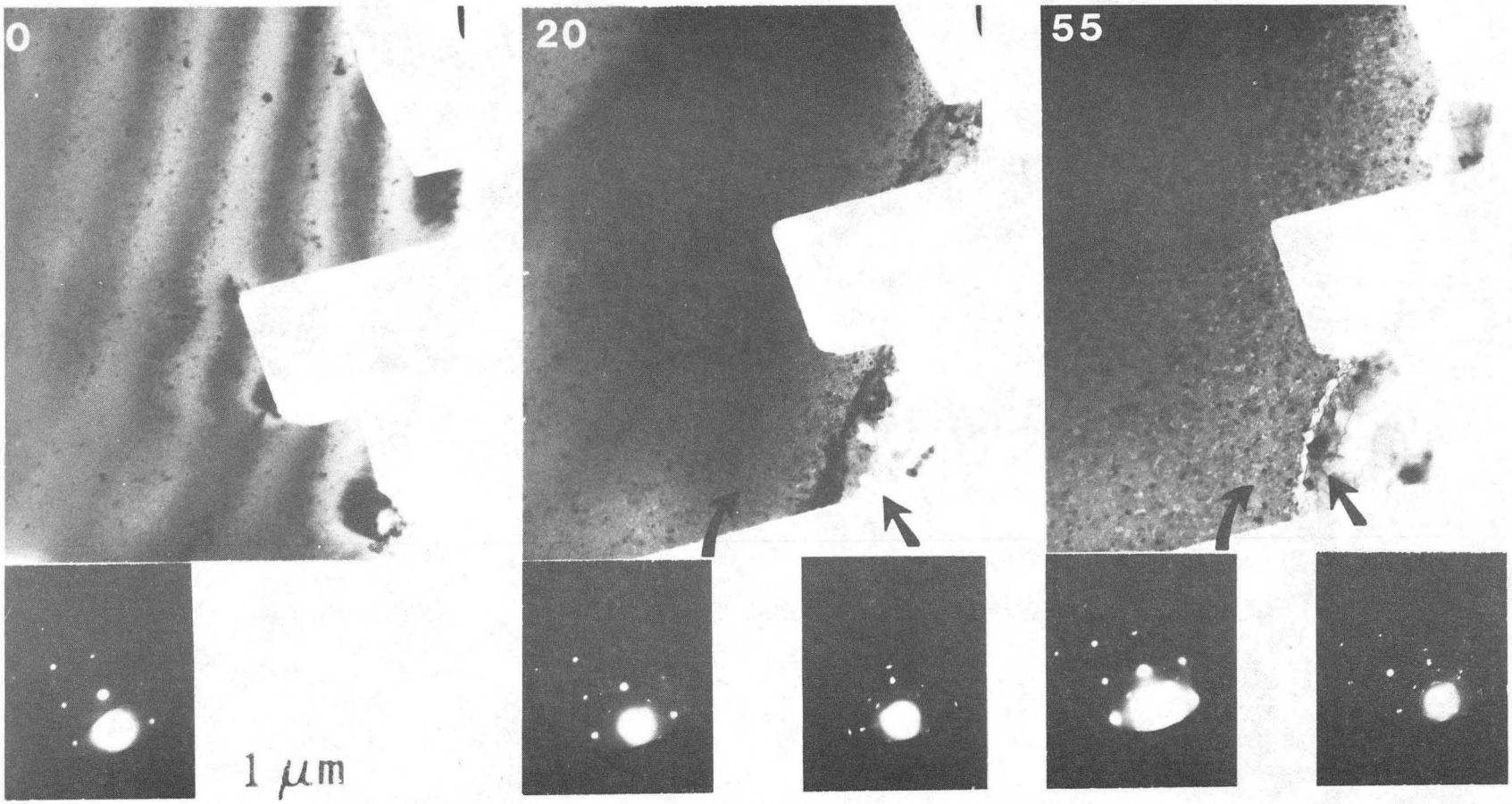

XBB 869-7870

Fig. 7

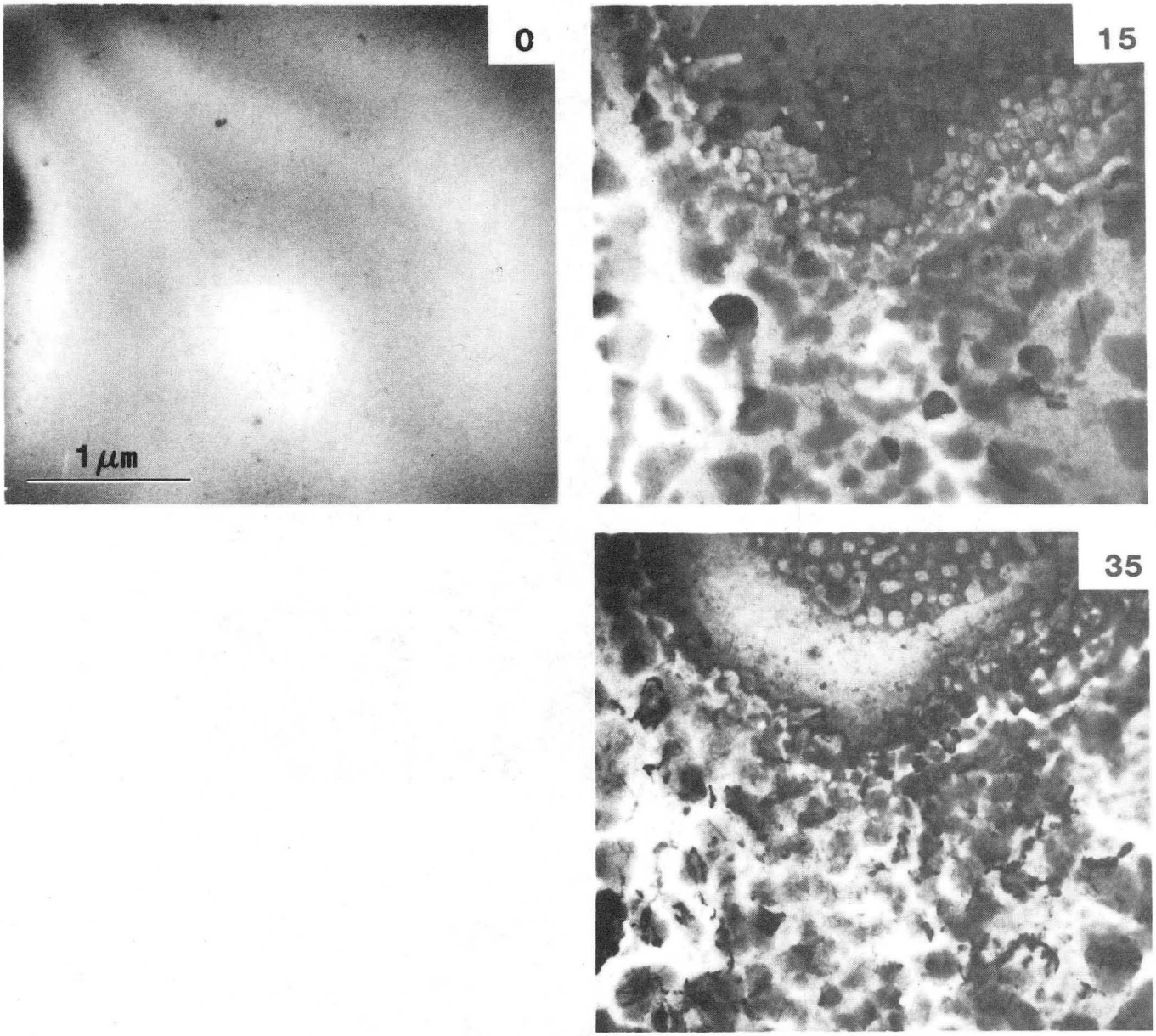

XBB 869-7874

Fig. 8

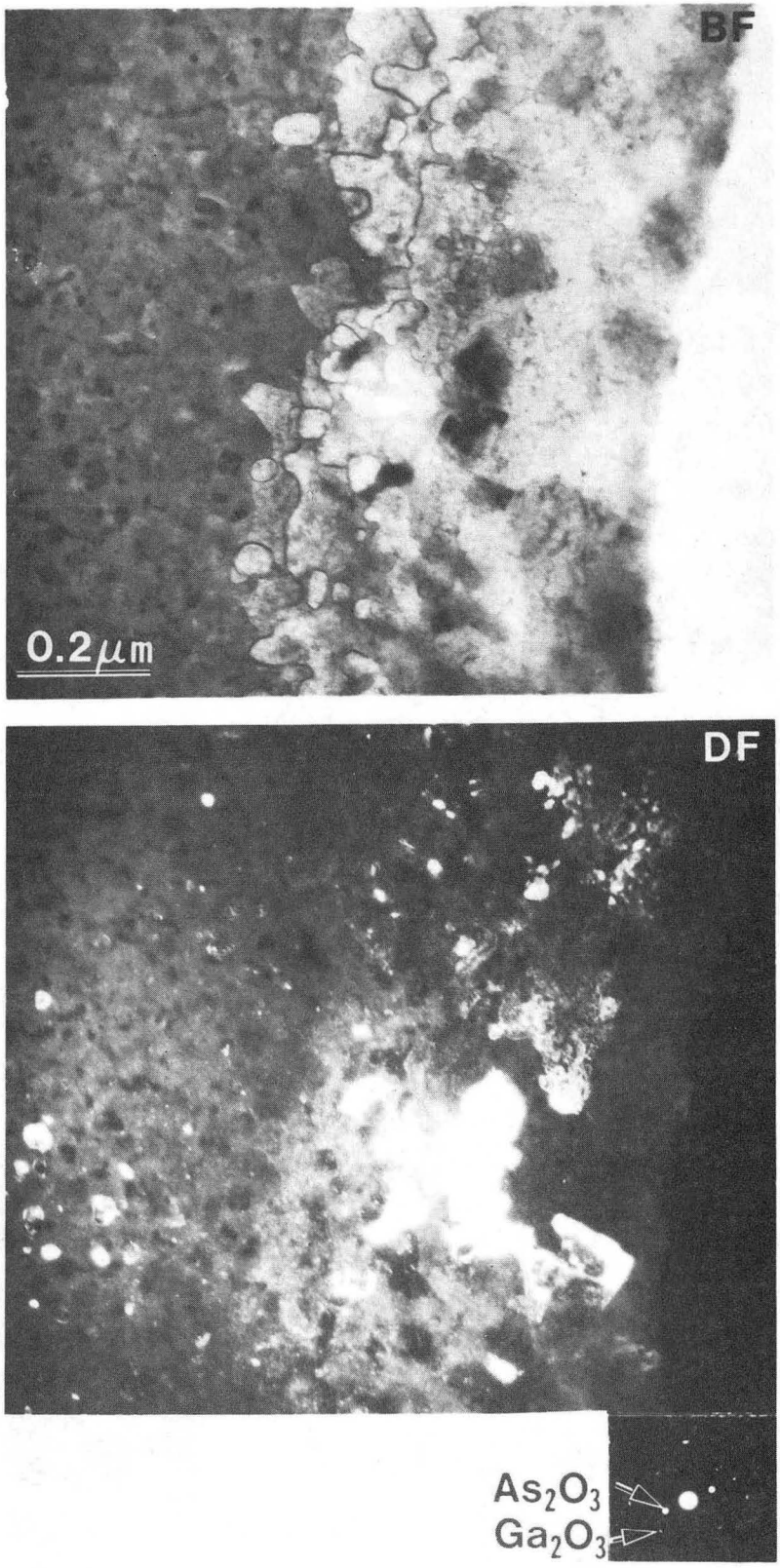

XBB 869-7884

Fig. 9

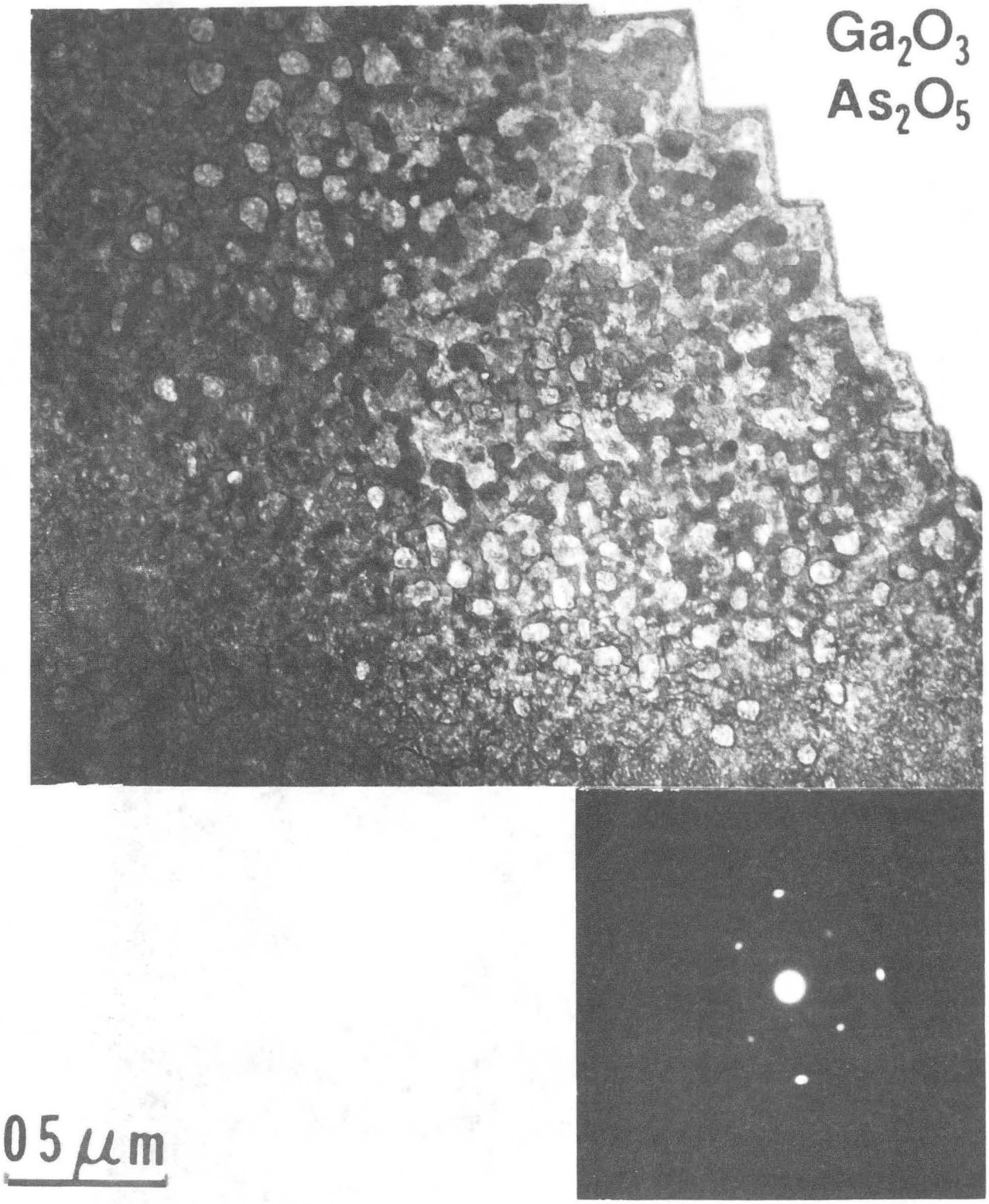

XBB 869-7830

Fig. 10

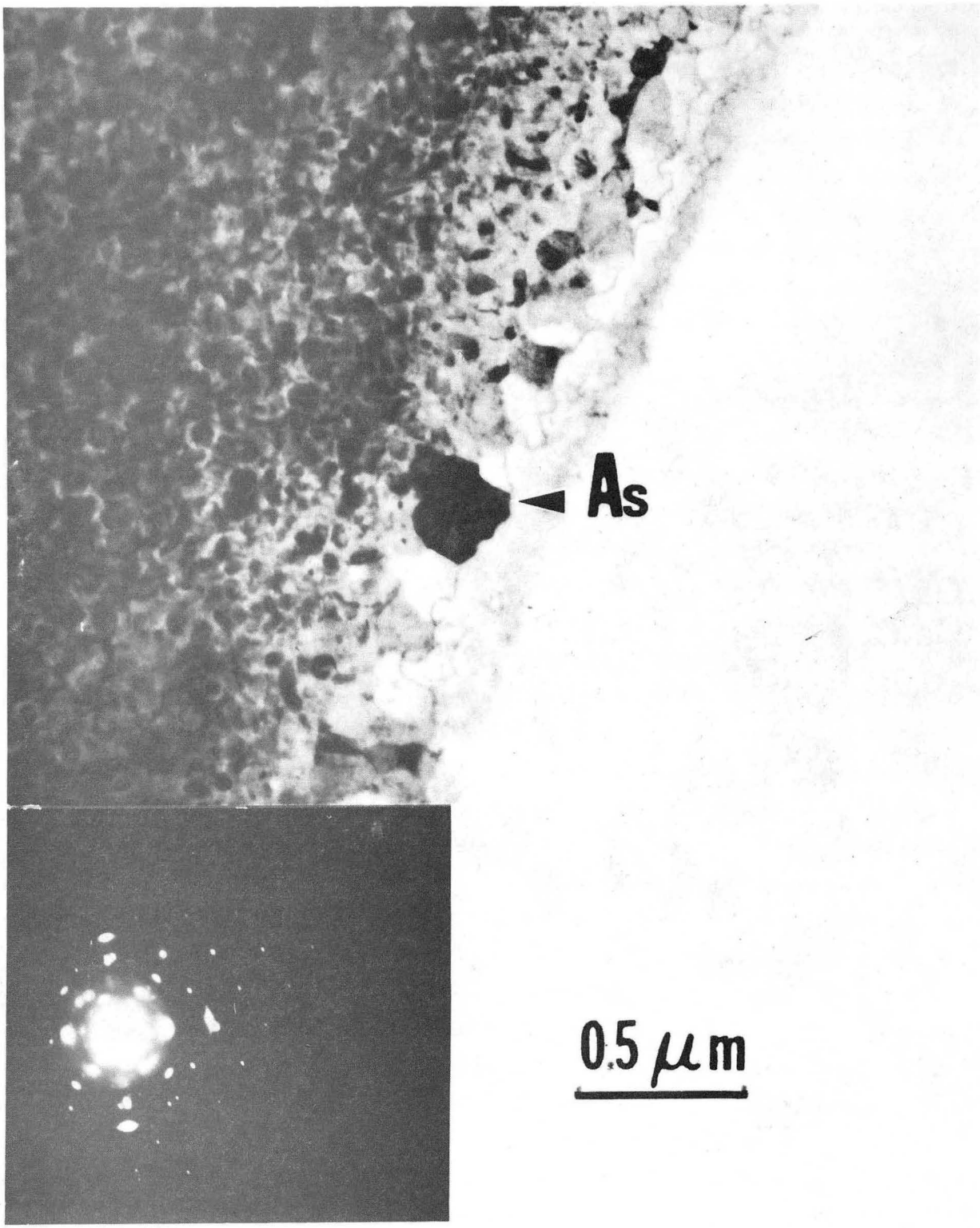

XBB 869-7881

Fig. 11

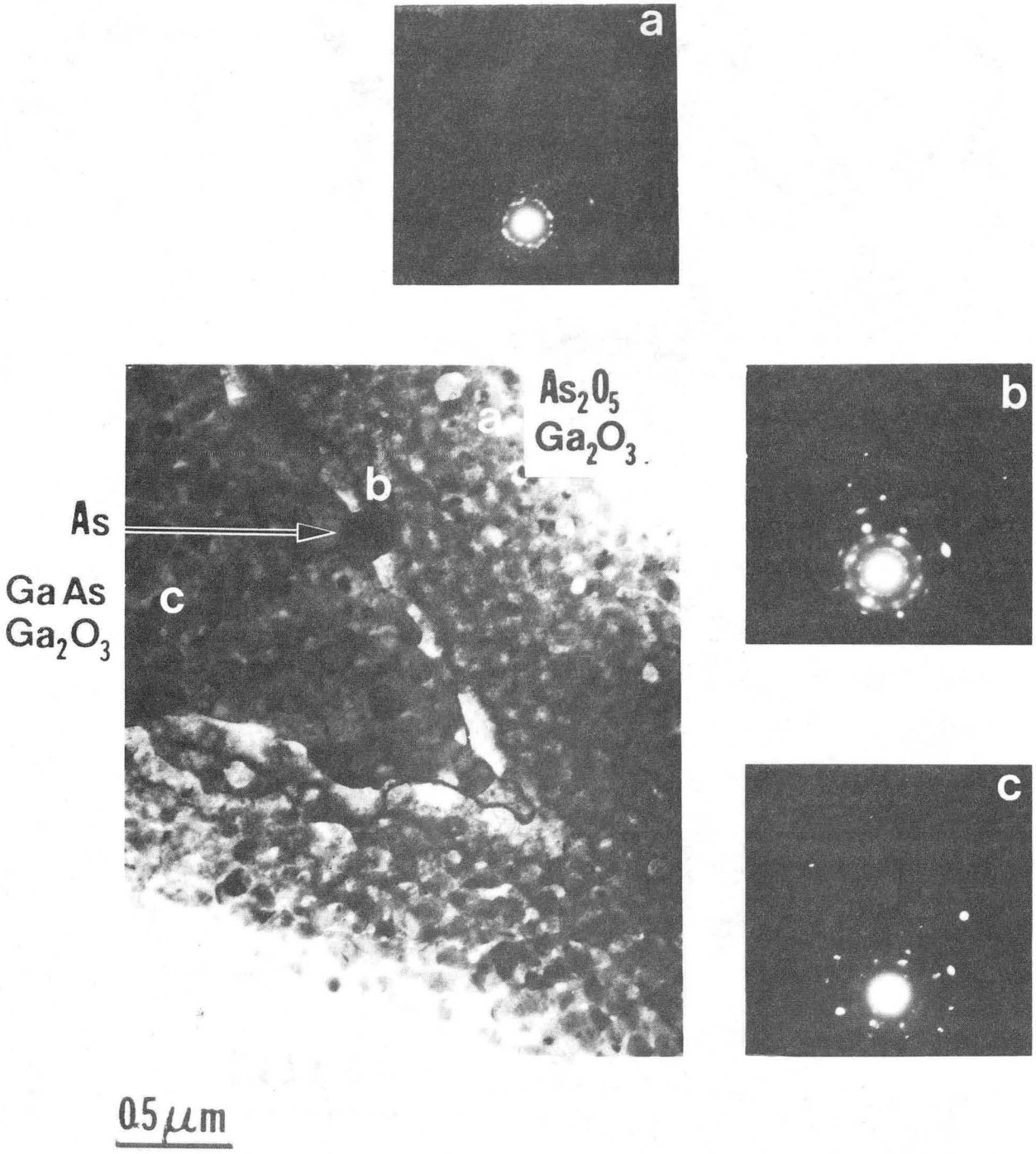

XBB 869-7877

Fig. 12

a

b

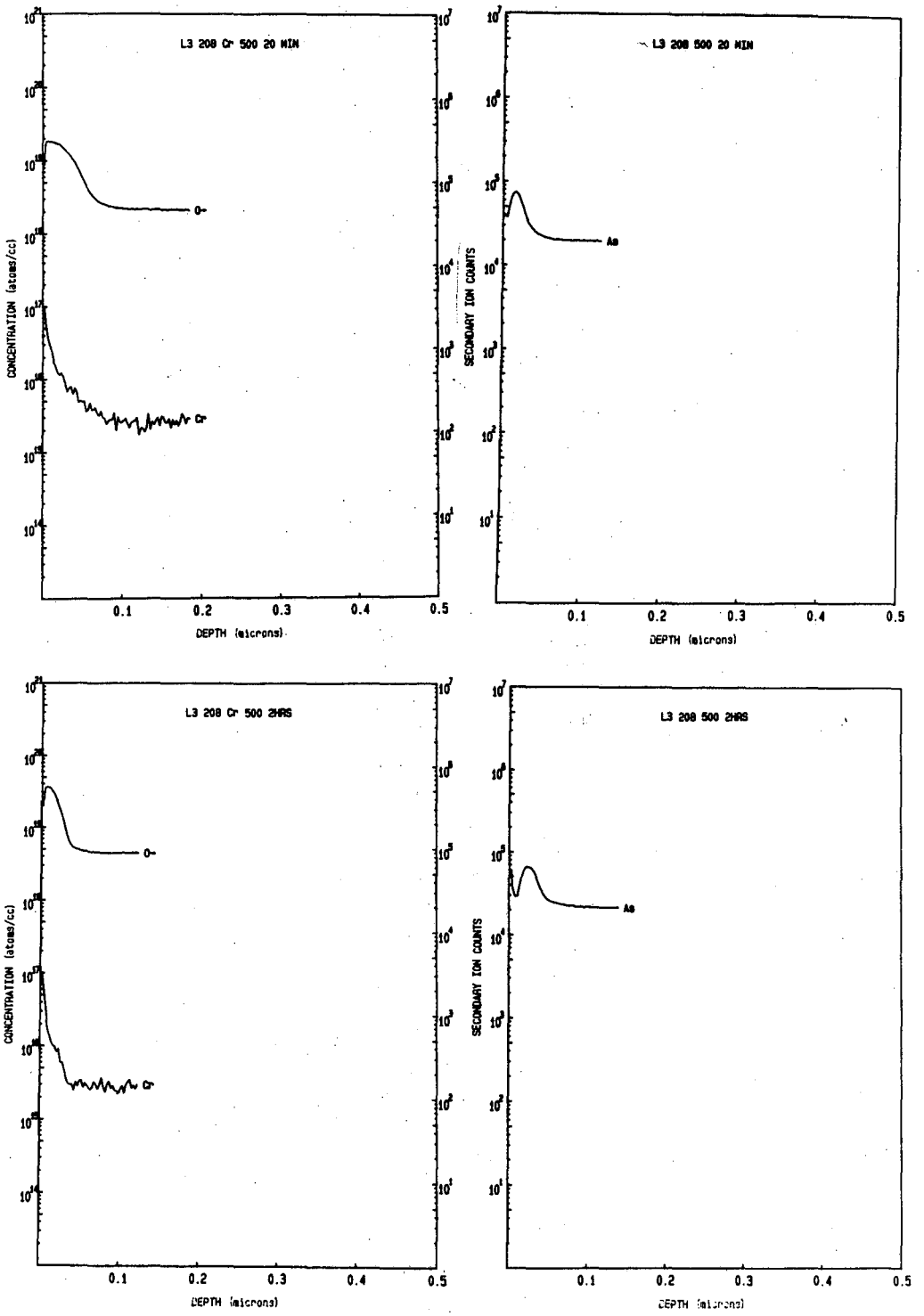
L3 208 Cr 500 20 MIN
L3 208 500 20 MIN
L3 208 Cr 500 2HRS
L3 208 500 2HRS
CONCENTRATION (atoms/cc)
SECONDARY ION COUNTS
DEPTH (microns)
O-
Cr
As

Fig. 13

c

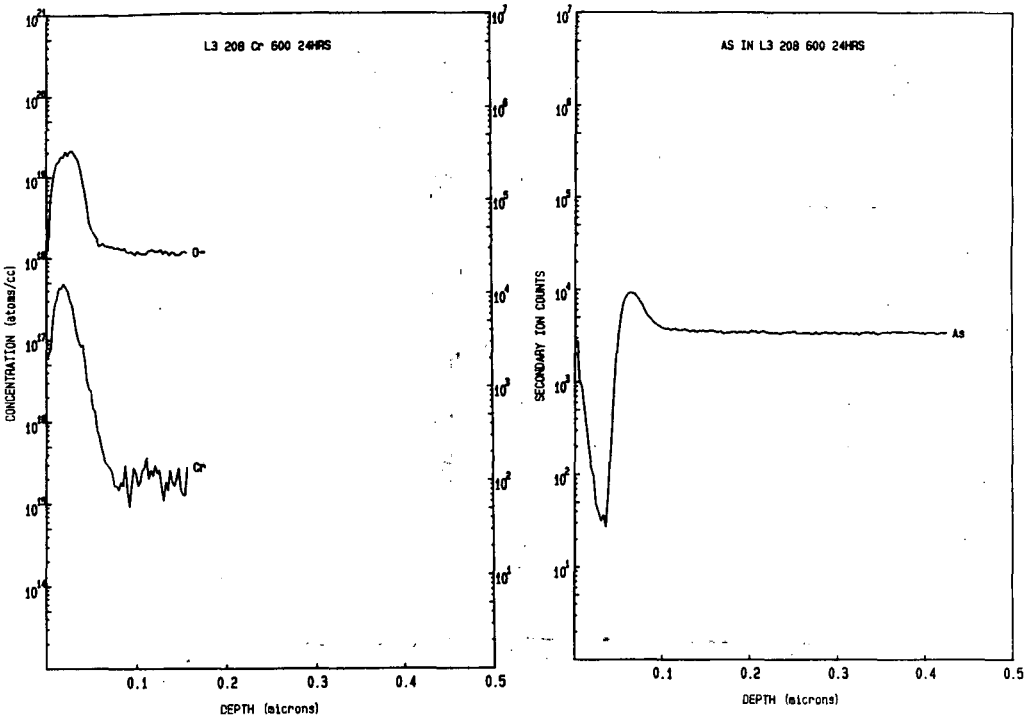
L3 208 Cr 600 24HRS
CONCENTRATION (atoms/cc)
O-
Cr
DEPTH (microns)
AS IN L3 208 600 24HRS
SECONDARY ION COUNTS
As
DEPTH (microns)

Fig. 13c

This report was done with support from the Department of Energy. Any conclusions or opinions expressed in this report represent solely those of the author(s) and not necessarily those of The Regents of the University of California, the Lawrence Berkeley Laboratory or the Department of Energy.

Reference to a company or product name does not imply approval or recommendation of the product by the University of California or the U.S. Department of Energy to the exclusion of others that may be suitable.

LAWRENCE BERKELEY LABORATORY
TECHNICAL INFORMATION DEPARTMENT
UNIVERSITY OF CALIFORNIA
BERKELEY, CALIFORNIA 94720